# Effective crystal field and Fermi surface topology: A comparison of $d$- and $dp$-orbital models

N. Parragh,[1] G. Sangiovanni,[1] P. Hansmann,[2] S. Hummel,[3] K. Held,[3] and A. Toschi[3]

[1]*Institut für Theoretische Physik und Astrophysik, Universität Würzburg, Am Hubland, D-97074 Würzburg, Germany*
[2]*Centre de Physique Théorique, Ecole Polytechnique, CNRS-UMR7644, 91128 Palaiseau, Paris, France*
[3]*Institut für Festkörperphysik, Technische Universität Wien, 1040 Vienna, Austria*

The effective crystal field in multiorbital correlated materials can be either enhanced or reduced by electronic correlations with crucial consequences for the topology of the Fermi surface and, hence, on the physical properties of these systems. In this respect, recent local density approximation plus dynamical mean-field theory studies of Ni-based heterostructure have shown contradicting results, depending on whether the less correlated $p$ orbitals are included or not. We investigate the origin of this problem and identify the key parameters controlling the Fermi surface properties of these systems. Without the $p$ orbitals, the model is quarter-filled, while the $d$ manifold moves rapidly towards half-filling when the $p$ orbitals are included. This implies that the local Hund's exchange, while rather unimportant for the former case, can play a predominant role in controlling the orbital polarization for the extended basis set by favoring the formation of a larger local magnetic moment.

PACS number(s): 71.10.−w, 71.27.+a, 73.40.−c

## I. INTRODUCTION

Correlated electronic systems display some of the most fascinating phenomena in solid state physics. One of their typical characteristics is a strong sensitivity to small changes of external control parameters. Hence, a precise understanding of the underlying physics and of the pivotal parameters controlling the observed phenomenology represents a crucial goal in contemporary condensed matter research, also in light of possible applications beyond the purely academic context.

The intrinsic complexity of many-body physics prevents an exact *ab initio* theoretical description of correlated materials. In fact, even one of the most basic models for electronic correlations, i.e., the Hubbard model[1] where only the local part of the Coulomb interaction is retained, can not be exactly solved in the relevant cases of two or three dimensions. However, a great step forward in the theoretical analysis of electronic correlation in condensed matter was achieved in the last decades by means of dynamical mean-field theory (DMFT),[2,3] and, for realistic material calculations, by its merger with *ab initio* density functional approaches such as the local density approximation (LDA + DMFT).[4]

From the theoretical point of view, DMFT-based methods can be viewed as a quantum extension of the classical mean-field approaches. Hence, the application of DMFT implies neglecting all nonlocal spatial correlations albeit allowing for a very accurate (and nonperturbative) treatment of the most relevant part of the electronic correlations stemming from the (single or multiorbital) Hubbard interaction, i.e., their purely local part. The ability of DMFT to capture these local quantum fluctuations is one of the keys behind its success in addressing many open questions in the physics of strongly correlated materials. Among those, we recall the pioneering DMFT description of the Mott[5] metal-insulator transition (MIT) in $V_2O_3$,[3,6] of the $\delta$ phase of Pu,[7] of the correlation effects[8] in Fe and Ni, of the volume collapse in Ce,[9] of the unconventional pairing mechanism of superconductivity in fullerenes;[10] most recently, DMFT has been also successfully applied to the analysis of the occurrence of kinks in the self-energy[11] and in

the specific heat[12] of particular vanadates, such as $SrVO_3$, and $LiV_2O_4$, as well as of the spectral and magnetic properties[13,14] of Fe-based superconductors.

Furthermore, it should also be recalled here that DMFT is a very flexible scheme, whose application is possible also beyond the standard case of bulk correlated systems. In fact, DMFT-based methods have been recently used to study correlated nanoscopic[15] and hetero-structures.[16–18] For the latter case, we want to focus here, in particular, on the theoretical predictions for the Fermi surface properties of layered Ni-based heterostructures. The application of LDA + DMFT to this problem, and more specifically, to the case of a 1:1 layered $LaNiO_3$/$LaAlO_3$ heterostructure has raised a considerable interest, as the DMFT results of Refs. 18 and 19 clearly prospect the possibility to drive the Fermi surface "topology" of these materials very close to the one of the high-temperature superconducting cuprates. In fact, the electronic structure in the bulk nickelates, such as $R_{1−x}Sr_xNiO_4$, is typically characterized by *two* bands crossing the Fermi level,[20] which arise from the two $e_g$ orbitals of Ni (the "planar" $x^2 − y^2$ and "axial" $3z^2 − r^2$ orbitals). However, by growing heterostructures with planes of $LaNiO_3$ intercalated with insulating planes of $LaAlO_3$ and on substrates providing an epitaxial strain, such as $SrTiO_3$ or $PrScO_3$, the energetic configuration of the $3z^2 − r^2$ will be correspondingly disfavored,[21] which corresponds to a (by our definition positive) crystal field splitting $\Delta_{CF}^d = \varepsilon_{3z^2−r^2} − \varepsilon_{x^2−y^2} > 0$ among the two Ni $e_g$ orbitals. In this situation, LDA + DMFT calculations have shown that the inclusion of the correlation effects will always increase the original (LDA) crystal field splitting between the two $e_g$ orbitals,[22] leading, eventually, to a significant change of the "topology" of the Fermi surface, i.e., to a situation in which only *one* band, with predominant $x^2 − y^2$ character crosses the Fermi level. Hence, according to these LDA + DMFT calculations, in Ni-based heterostructures it would be possible to "artificially" realize the electronic configuration of the high-temperature superconducting cuprates (i.e., single, almost half-filled orbital with $x^2 − y^2$ symmetry close the Fermi level), e.g., by modulating

the strain through changing the substrate or the insulating layer. As the control of the low Fermi surface properties represents an essential ingredient for novel, alternative, realizations of high-temperature superconductivity, the importance of having highly accurate LDA + DMFT predictions becomes a crucial factor for engineering new materials.

In contrast to these impressive applications of DMFT-based methods, one important aspect should be stressed here: The LDA + DMFT procedure requires as an important step a downfolding to a chosen energy window around the Fermi energy $\varepsilon_F$. For most of the above mentioned studies, this window included only a few bands around $\varepsilon_F$ of dominant $3d$ character. In such a basis for the transition-metal oxides, the hybridization of $3d$ states and oxygen ligand $2p$ states is included *implicitly* in the effective bands. In the recent past, however, it has become customary to include the oxygen $2p$ states *explicitly*, i.e., to downfold to a larger energy window. In most of the cases, these additional ($p$) orbitals were way more extended than the correlated ones (e.g., $d$), and, hence, the local Coulomb interaction between electrons occupying these additional orbitals ($U_{pp}$) and between electrons on different manifolds ($U_{pd}$) was either completely neglected, or, in some exceptional cases, treated at the Hartree level.[25] Despite this approximation, it is quite intuitive to expect that the validity of LDA + DMFT calculations performed in an enlarged (say, $dp$) basis set is more general than the corresponding one in the restricted $d$ manifold. In fact, quite generally, (i) performing a renormalization [Wannier[26] projection, $N$th-order muffin-tin orbital (NMTO) (Ref. [27]) downfolding, etc.] on an enlarged basis set allows for a better localization of the orbitals of the correlated manifold (as the $dp$-hopping processes are now explicitly included in the model); and (ii) the possibility of describing explicitly charge-transfer processes between the $d$ and $p$ orbitals makes the theoretical modeling evidently closer to the actual material physics.[28]

Notwithstanding these quite general arguments, the improvement of LDA + DMFT calculations on enlarged $dp$ basis sets w.r.t. the ones restricted to effective $d$-only basis, is not always apparent. In fact, there are cases for which a treatment on a larger basis set renders the comparison with experiment to be worse! Without attempting to give a complete review here, we recall that LDA + DMFT calculations including $p$ orbitals have improved the descriptions of the insulating behavior of NiO (Ref. [29]) and of the MIT in NiS$_2$ (Ref. [30]) w.r.t. $d$-only calculations.[31] Also, quite accurate results have been obtained for one- and two-particle properties of cobaltates [such as SrCoO$_3$ (Ref. [32]) and LaCoO$_3$ (Ref. [33])] and in several studies[34] of the well-known class of iron pnictides and calchogenides.

In contrast to the aforementioned successful applications of $dp$ calculations, in other, equally important, cases the $dp$ LDA + DMFT results are in partial or total contradiction with the $d$-only calculations, and/or with the experimental findings: No MIT in V$_2$O$_3$ was found up to unrealistically large values of the Coulomb interaction if the oxygen $p$ orbitals are included in LDA + DMFT calculations.[35] More recently, also the Mott-Hubbard insulating phase of La$_2$CuO$_4$ and LaNiO$_3$ was reported to be missing in the $dp$ framework,[36] while these materials are found to be insulating in $d$-only calculations for plausible values of the $dd$ interaction. These discrepancies between $d$-only and $dp$ calculations regarding the Mott-Hubbard MIT have already raised a discussion in the recent literature. In Ref. [36], nonlocal correlations to be included beyond DMFT (Ref. [37]) have been considered as a cause of the discrepancy. In fact, a major role of spatial correlations in determining the onset of insulating phases is quite likely, especially in the case of two-dimensional cuprates.

However, there are also other discrepancies, whose discussion will be the object of this work, which can be hardly attributed to the effects of nonlocal correlations. These discrepancies are observed for systems of more than one correlated $d$ orbital and in broad parameter regimes (including high temperatures), where effects beyond DMFT should not play a crucial role. In particular, a striking disagreement between $d$-only and $dp$ calculations was reported for the above-mentioned case of Ni-based heterostructures. In fact, LDA + DMFT calculations performed including also the oxygen $p$ orbitals have shown[38] exactly the opposite trend w.r.t. the previous ones: Even in the presence of a favorable crystal field splitting $\Delta_{CF}^d = \varepsilon_{3z^2-r^2} - \varepsilon_{x^2-y^2} > 0$ at the starting (LDA) level, the net effect of the Hubbard interaction was *always* to reduce the orbital polarization by filling back the $3z^2 - r^2$ orbital, which would prohibit *de facto* any possibility of realizing the cuprate conditions for the onset of an unconventional superconductivity.

This second kind of discrepancies between LDA + DMFT performed with different ($d$-only versus $dp$) basis sets well illustrated by the contradicting results for the Ni-based heterostructures raises a quite general question about the proper use and interpretation of the growing number of LDA + DMFT calculations on extended basis sets. The correct determination of the orbital polarization and Fermi surface properties is of great importance for future calculations of increasingly complex materials.

In this paper, we aim at understanding the relations between the results of existing LDA + DMFT calculations on different basis sets for the Fermi surface properties of multiorbital systems and, ultimately, the origin of the qualitative discrepancies observed by following the standard implementation of the algorithms in different basis sets. For this purpose, it is of primary importance to disentangle the main, qualitative, trends from the specific features of a selected case. Hence, we will study model Hamiltonians for different crystal field splittings starting from a $dp$ basis (four bands). Subsequently, we perform a downfolding to an effective $d$-only basis and compare DMFT ressults of both cases. This procedure will capture the above-mentioned discrepancy in the prediction of Fermi surfaces of correlated multiorbital systems and allow for a systematic study of this problem in the context of Ni-based materials.

The scheme of the paper is the following: In Sec. II, we introduce the models. In Sec. III, we analyze the disagreement in the calculation of the orbital occupations and the shape of the Fermi surfaces between $d$-only and $dp$ models for a fixed set of interaction parameters. At the end of Sec. III, we also provide an analysis of the role of Hund's exchange $J$. In Sec. IV, we study the origin of the observed inconsistencies by analyzing the dependence on the $d$-electron density, and we discuss its possible relation with the crossover[39] from high spin (Hund's regime) to low spin (CF regime). Finally, in Sec. V, we summarize our results.

## II. MODELS AND METHODS

In this section, we illustrate the simplified model Hamiltonians chosen to analyze the discrepancies between the existing LDA + DMFT calculations on different ($d$-only versus $dp$) basis sets for the prediction of the orbital polarization and the Fermi surface properties of correlated multiorbital systems. Let us stress that, in this work, we aim at a basic understanding of the general physics underlying the contradicting outcomes of realistic calculations, rather than discussing the case of a specific material. As a guidance for the choice of the model, we recall (see Sec. I) that important inconsistencies in the theoretical predictions emerged already when considering the presumably simple case of two correlated (namely, $e_g$)[40] orbitals only, such as in the case of bulk nickelates[20] and Ni-based heterostructures.[18,19,38]

Hence, we will introduce here two models (distinguished for the different basis sets), built with tetragonal symmetry, allowing for the simplest realization of the above-mentioned situation of two correlated orbitals (identified with the two $e_g$ $d$ orbitals) in the presence of a minimal number of extended ligand orbitals (henceforth associated to $p$ orbitals). The models are inspired, to some extent, by the realistic calculations of nickelate heterostructures, i.e., with a focus on the orbital polarization in a quasi-two-dimensional geometry. However, we will not consider here spatial correlations beyond DMFT,[37] the "dimensionality" entering explicitly only via the $k$ summations defining the local quantities. Therefore, the results will depend mainly on the "effective" crystal field splitting, on the orbital occupation, and on the electronic kinetic energies. Furthermore, the general trends emerging from our DMFT calculations are found to be stable w.r.t. the specific parameter choice of the $dp$ and $d$-only models we are going to consider. Hence, our study will provide useful indications to identify and clarify the global trends of the multiorbital physics of this class of systems, *at the DMFT level*.

Specifically, the model Hamiltonians considered will be the following:

(1) The one-particle model Hamiltonian for the larger basis set, from which we start conceptually, is a $dp$ four-band model (Fig. 1 upper panels), that includes explicitly two correlated

$d$ orbitals (e.g., the nickel 3$d$ $e_g$ states), and two ligand (e.g., oxygen 2$p$ states).

(2) The model for the smaller basis set is the (Löwdin) downfolded[41,42] version of the first one on the two correlated (e.g., 3$d$ $e_g$) orbitals: It corresponds to the two-orbital $d$-only band structure, shown with the corresponding orbital character in Fig. 1 (lower panels).

Note that, due to the downfolding, the band structure of the two models at the Fermi level is identical by construction. Yet, the associated orbital character is different.

### A. $dp$ four-band model

While DMFT calculations are often performed first in the smallest possible basis set, for the definition of our one-particle model Hamiltonians it is conceptually more logical to start from a larger ($dp$) basis set. In our case, this includes two correlated $d$ orbitals and two ligand $p$ orbitals. The specific dispersion considered corresponds to a quasi-two-dimensional geometry of the model, which can be thought of as one $p_x$ and one $p_y$ orbital on each ligand site. The overlap between the ligand orbitals and the two $e_g$ orbitals gives the largest contribution to the hopping processes ($t_{pd}$). Hence, for the sake of simplicity, the smaller direct hopping among $d$ orbitals is neglected ($t_{dd} = 0$). Furthermore, in our one-particle Hamiltonian, the $d$ and the $p$ manifolds are kept well distinguishable, in that a large enough $dp$ splitting is assumed (see below for details). These choices correspond to the minimal $dp$ model with a realistic $dp$ configuration in a (quasi-two-dimensional) cubic/tetragonal symmetry.

The specific values of the parameters, e.g., the $dp$-hopping amplitude ($t_{pd}$), onsite $d/p$ energies, and crystal field splitting among the $d$ orbitals ($\Delta_{CF}$) have therefore been chosen to obtain a reasonable bandwidth for the bands close to the Fermi level. Our choice also ensures that the positive/negative values assumed by the splitting $\Delta_{CF}^d$ between the two downfolded $d$ orbitals in the small basis set are plausible. This way, we build up a one-particle low-energy Hamiltonian similar to the four-band cuprate Hamiltonian derived in Ref. 43, whereas the role of our "axial" orbital $3z^2 - r^2$ is played by the 4$s$ orbital of Cu. Formally, our $dp$ Hamiltonian in momentum space reads as

$$H_{\mathbf{k}}^{4b} = \begin{pmatrix} 0 & 0 & i\sqrt{3}t_{pd}\sin\left(\frac{k_x}{2}\right) & -i\sqrt{3}t_{pd}\sin\left(\frac{k_y}{2}\right) \\ 0 & \Delta_{CF} & it_{pd}\sin\left(\frac{k_x}{2}\right) & it_{pd}\sin\left(\frac{k_y}{2}\right) \\ -i\sqrt{3}t_{pd}\sin\left(\frac{k_x}{2}\right) & -it_{pd}\sin\left(\frac{k_x}{2}\right) & \epsilon_p & 0 \\ i\sqrt{3}t_{pd}\sin\left(\frac{k_y}{2}\right) & -it_{pd}\sin\left(\frac{k_y}{2}\right) & 0 & \epsilon_p \end{pmatrix}, \quad (1)$$

where the lattice spacing $a = 1$, $t_{dp} = 1.8$ eV, and $\Delta_{CF} = [0.7, 1.7]$ eV ($\Delta_{CF}^d = [-0.53, +0.37]$ eV) for the reason explained above. The onsite energy of the $p$ states was fixed to $\epsilon_p = -2.5$ eV, similar to the position of the $p$ bands in the nickelate systems. As for the Fermi level, the model is assumed to have typically overall filling of five electrons. This would

correspond, ideally, to the situation of filled ligand bands and to a quarter-filled correlated two-band manifold at the Fermi level.

In the lower panels of Fig. 1, we show the band structure of the four-band $dp$ model corresponding to the two extreme values of $\Delta_{CF}$ we considered. In the band structure and
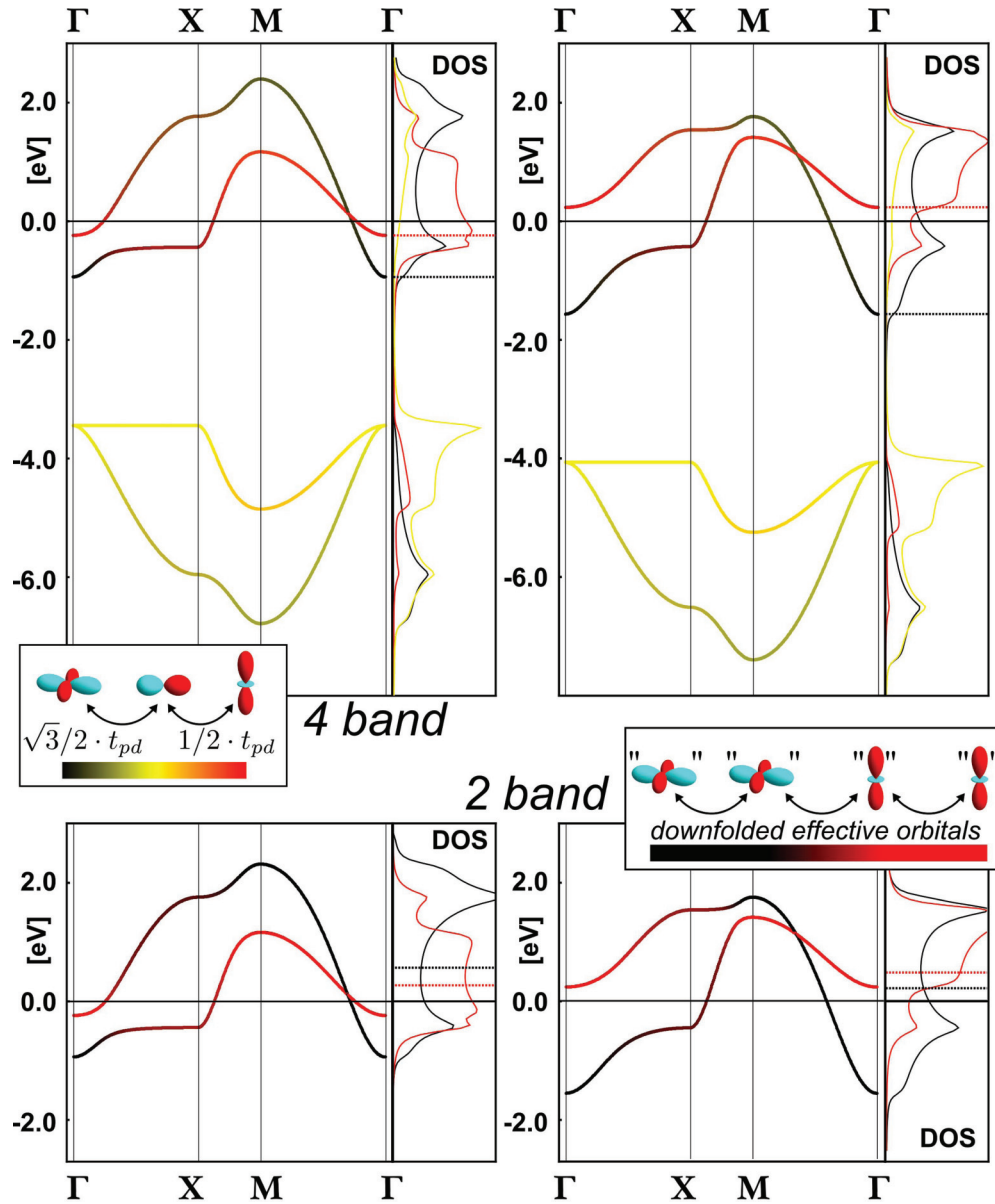
FIG. 1. (Color online) Band structure and DOS of the four-band $dp$ model (upper panel) and the corresponding downfolded two-band $d$-only model (lower panel) for two different values of the crystal field splitting $\Delta_{\mathrm{CF}}$ between the $e_g$ orbitals of the $dp$ Hamiltonian [Eq. (1)]. Specifically, these are $\Delta_{\mathrm{CF}} = 0.7$ eV (left panels) and 1.7 eV (right panels), corresponding to a local energy splitting $\Delta^d_{\mathrm{CF}} = -0.53$ and 0.37 eV, respectively, in the $d$-only model. The orbital character is denoted by the following color coding: black for the first $d$ orbital ($x^2 - y^2$), red for the second ($3z^2 - r^2$), and yellow for the $p$ orbitals. In the inset, the hopping processes for the two models are sketched.

DOS plots, the black/red color encodes the $d$ character ($x^2 - y^2/3z^2 - r^2$, respectively), and the yellow color encodes the $p$ character.

### B. *d*-only two-band model

The $d$-only model has been obtained by means of a Löwdin downfolding of the $dp$ Hamiltonian (1) which means that their respective electronic structure at the Fermi level is identical by construction. The overall result of the downfolding procedure is reported in the corresponding orbitally resolved band structure for the two-band model in Fig. 1 (bottom panels). Specifically, the band structure and DOS of Fig. 1 have been obtained by downfolding the $dp$ Hamiltonians

with the lowest and the highest values of $\Delta_{\mathrm{CF}}$ (and $\Delta^d_{\mathrm{CF}}$), respectively. The orbital occupation of the $d$-only model has been fixed to $n_d = 1$ (quarter-filling).

In Fig. 1, the color code denotes, similarly as before, the orbital character: black and red represent the downfolded $x^2 - y^2$ and $3z^2 - r^2$ orbitals, respectively. At a closer inspection of the figure, we note that, while locally the two $e_g$ orbitals are eigenstates of the tetragonal point group and do not hybridize (pure black/red color of the DOS), they do obviously hybridize nonlocally along certain directions (dark red color, e.g., at the $X$ point of the Brillouin zone). Furthermore, we observe that the overall width (as well as the associated kinetic energy) of the $3z^2 - r^2$ DOS is smaller than the $x^2 - y^2$ one, a typical feature of anisotropic materials

and/or heterostructures with a quasi-two-dimensional hopping geometry with suppressed hopping along the $c$ axis. More importantly for our purposes, we stress how the different original values of $\Delta_{CF}$ in the $dp$ basis sets correspond to situations with negative/positive difference between the center of mass of the noninteracting DOS of our $d$-only model. Specifically, this means that the important parameter $\Delta_{CF}^{d} = \varepsilon_{3z^2-r^2} - \varepsilon_{x^2-y^2}$, accounting for the onsite energy difference[45] between the two $e_g$ states *in the downfolded model*, will be varying in the range of $[-0.53, 0.37]$ depending on the chosen value of $\Delta_{CF}$ in the starting $dp$ Hamiltonian. We stress here that $\Delta_{CF}^{d}$ can be interpreted, to a certain extent, as "crystal field" within the $d$-only manyfold. However, by adopting such a "rough" definition, one should keep in mind that $\Delta_{CF}^{d}$ is, in fact, a "ligand field" splitting, originated by an electrostatic Madelung potential *and* a $dp$-hybridization splitting.

Before discussing some technical aspects of our DMFT implementation in the next section, we recall that related two-band model Hamiltonians, but *without* hybridization between the $d$ orbitals, have been studied with DMFT in Ref. 39, with reference to the cases of $BaVS_3$ and $Na_xCoO_2$.

### C. DMFT algorithm in extended basis sets

The DMFT algorithm applied to a chosen correlated orbital subspace, possibly derived from *ab initio* calculations, has already become a quite standardized procedure (for details, we refer the reader to Ref. 4). However, in consideration of the discrepancies appearing when extending the basis set by including less-correlated ligand $p$ orbitals in the self-consistent DMFT loop, we will explicitly recall here some technical aspects of the DMFT algorithmic procedure usually adopted in the cases of the extended $dp$ basis sets.

Extended models including ligand $p$ states explicitly have a structure like our four-band Hamiltonian (1). Locally, i.e., integrated over the Brillouin zone, such Hamiltonian has the form

$$H_{\text{full}}^{\text{loc.}}(R=0) = \begin{pmatrix} H_{dd}^{\text{loc.}} & H_{dp}^{\text{hyb.}} \\ \left(H_{dp}^{\text{hyb.}}\right)^{\dagger} & H_{pp}^{\text{loc.}} \end{pmatrix}. \tag{2}$$

The local basis is typically chosen in a way that the $H_{dd}$ and $H_{pp}$ blocks can be made internally diagonal after **k** integration so that the states can be labeled by a good *local* quantum number in the respective subspaces, such as the crystal field labels (see DOS plots in Fig. 1). In such a basis, the local Coulomb ($U$) matrix of the interacting part of the Hamiltonian is then defined - in its SU(2)-invariant "Kanamori" - form as

$$H_{\text{loc.}} = \sum_{a} U n_{a,\uparrow} n_{a,\downarrow}$$
$$+ \sum_{a>b,\sigma} [U' n_{a,\sigma} n_{b,-\sigma} + (U'-J) n_{a,\sigma} n_{b,\sigma}]$$
$$- \sum_{a \neq b} J(d_{a,\downarrow}^{\dagger} d_{b,\uparrow}^{\dagger} d_{b,\downarrow} d_{a,\uparrow} + d_{b,\uparrow}^{\dagger} d_{b,\downarrow}^{\dagger} d_{a,\uparrow} d_{a,\downarrow} + \text{H.c.})$$

for the $d$-orbital sector. Here, $U$ denotes the interaction parameter between two electrons in the same $d$ orbital, $U'$ the interaction between electrons on different $d$ orbitals, and $J$ is the Hund's coupling; $a,b$ index the two orbitals and $\sigma$ the spin. Note that the specific interaction values for the DMFT

calculations (see next section for details) have been chosen in order to reproduce a typical correlated metallic situation. Due to the stronger localization of the $d$ orbitals in the $dp$ models, the corresponding values of the local interaction on the $d$ orbitals have been correspondingly enhanced (we assumed here a factor 2 for the parameter $U'$). We recall that, for the $dp$ case, the multiorbital Hubbard interaction could include, aside from onsite $d$ and onsite $p$ interactions, also possible $dp$ interactions. This is, however, not the topic of this study. Furthermore, for the $dp$ model in LDA + DMFT, we have to face the so-called problem of *double-counting correction* (DC) (Refs. 4,46, and 47): Unlike for a $d$-only model, this does not correspond to a simple total energy shift and, hence, can not be "absorbed" in the chemical potential. The DC for the $dp$ models corresponds to a renormalization of the energy difference between $d$ and $p$ states. For our models, we have used the DC suggested by Anisimov,[46] given by

$$\bar{U}_{dd} = [U + U'(N_d - 1) + (U' - J)(N_d - 1)]/(2N_d - 1),$$

$$\Delta_{DC} = \bar{U}_{dd}\left(\sum_d n_d^{\text{LDA}} - \frac{1}{2}\right), \tag{3}$$

where $N_d$ is the number of $d$ orbitals, and $\bar{U}_{dd}$ is the average local interaction between these $d$ orbitals; $n_d^{\text{LDA}}$ denotes the occupation of the $d$ orbitals as calculated from the **k**-resolved noninteracting (LDA) Hamiltonian discussed above.

The self-consistent DMFT loop, which includes the solution of an Anderson impurity problem for the correlated subspace at each step, is done as follows:

(1) The first step is the calculation of the **k**-integrated Green's function on the *full $dp$* basis set:

$$G_{\text{full}}^{\text{loc.}}(\omega) = \frac{1}{V_{\text{BZ}}} \int_{\text{BZ}} d^3k \left[(\omega + \mu)\mathbb{1} - H_{\mathbf{k}}^{\text{4b}} - \Sigma_{\text{full}}(\omega)\right]^{-1}, \tag{4}$$

where $G$, $\Sigma_{\text{full}}$, and $H_{\mathbf{k}}$ are matrices in the $dp$ basis.

(2) Next, we extract the $dd$ block of the local Green's function:

$$G_{dd}^{\text{loc.}}(\omega) = \left\{G_{\text{full}}^{\text{loc.}}(\omega)\right\}\big|_{dd\,\text{block}}, \tag{5}$$

i.e., we project it onto the $d$ subspace. We stress here, that due to the $dp$ hybridization encoded in the Hamiltonian $H_{\mathbf{k}}^{\text{4b}}$ and the inversion of Eq. (4) the information about the $p$ ligands is not lost but captured by $G_{dd}^{\text{loc.}}(\omega)$.

(3) Now, in complete analogy to DMFT for $d$ states only, we calculate the Weiss field for the impurity model (only on the $d$ subspace):

$$[\mathcal{G}^0(\omega)]^{-1} = [G_{dd}(\omega)]^{-1} + \Sigma_{dd}^{\text{DMFT}}(\omega), \tag{6}$$

where $\Sigma_{dd}^{\text{DMFT}}(\omega)$ denotes the DMFT $dd$ self-energy.

(4) With $\mathcal{G}^0(\omega)$ we solve the auxiliary impurity problem (see below), obtain a new impurity Green's function and a new self-energy for the $d$ orbitals. Finally, the self-consistent loop is closed by comparing both the new and the old $\Sigma_{dd}^{\text{DMFT}}(\omega)$ *and* the new and the old $d/dp$ density and iterating until convergence.

As impurity solver for our DMFT calculations, we have used the continuous time quantum Monte Carlo (QMC) algorithm in the hybridization expansion (CT-HYB),[48,49] which

allows also for the treatment of the spin-flip and pair-hopping terms of our Kanamori Hamiltonian (3). In the CT-HYB, the time evolution is calculated using the local interaction, which makes the local Hilbert space growing exponentially with the number of orbitals. While for density-density interactions this problem can be mitigated along the line of Refs. 48 and 50, for the more realistic Kanamori interaction a set of quantum numbers, called PS, leads to a more efficient algorithm.[51] We have used this to perform all calculations presented in this paper with the full SU(2)-symmetric Hamiltonian.

## III. RESULTS: *d* VS *dp* CALCULATIONS AT "QUARTER-FILLING"

In this section, we compare our DMFT results obtained in the two different basis sets. Following the chronological order of appearance of realistic LDA + DMFT calculations for these systems, we present data for the *d*-only (downfolded) basis set first and then the corresponding ones for the original *dp* Hamiltonian.

We mention that our model study can be qualitatively related, depending on the initial value of the energy splitting between the correlated orbitals ($\Delta_{\text{CF}}^d = \varepsilon_{3z^2-r^2} - \varepsilon_{x^2-y^2}$), to the physics of bulk nickelates[20] and of Ni-based heterostructures.[18,19,38] In fact, (i) the nominal charge of these systems corresponds also to one electron in the outer two Ni bands and (ii) the bulk nickelates are typically characterized by negative values of $\Delta_{\text{CF}}^d$, due to the tetragonal distortion along the *z* axis. In the Ni-based heterostructures instead, the localization effects in the *z* direction, as well as the epitaxial strain due to the substrate, induce positive values for $\Delta_{\text{CF}}^d$.

### A. DMFT results for the (downfolded) *d*-only model

In this section, we analyze the results for our *d*-only two-orbital model at quarter-filling ($n_d = 1$), as a function of the initial energy splitting between the two downfolded $e_g$ orbitals ($\Delta_{\text{CF}}^d$): the corresponding results for the orbital occupation without interaction (which would correspond to the LDA ones, in a realistic calculation) and with the interaction (computed with DMFT) are shown in Fig. 2. As mentioned in Sec. II, the interaction values have been chosen in consideration of typical values for transition-metal oxides systems: for the *d*-only model, we adopted a value of $U' = U - 2J = 4$ eV, with $J = 0.75$ eV ($U = 5.5$ eV).

We start by briefly commenting the set of noninteracting data shown in Fig. 2: They display a clear-cut dependence on the initial value of the energy splitting of the $e_g$ orbitals: the orbital occupation of the $x^2 - y^2$ monotonously increases upon increasing values of $\Delta_{\text{CF}}^d$, whereas the occupation of the $3z^2 - r^2$ orbital decreases. We note, however, that, since the hopping terms (and, hence, the bandwidth) for the two orbitals are not equal, the orbital occupation curves are not symmetric w.r.t. to $\Delta_{\text{CF}}^d$. This also implies that the situation where the two orbitals are equally occupied (i.e., no orbital polarization) does not occur at $\Delta_{\text{CF}}^d = 0$ but, for the noninteracting case, only for $\Delta_{\text{CF}}^d \sim -0.4$ eV.

We discuss now the effects of the Hubbard interaction on the orbital occupations, as described by our DMFT(CT-QMC) calculations. While the occupation curves remain obviously
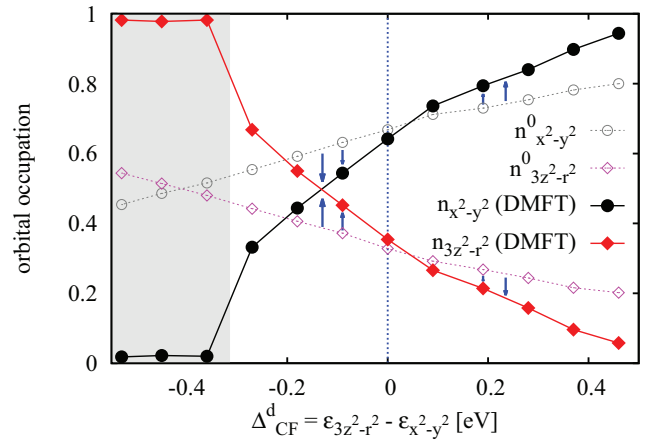


FIG. 2. (Color online) Orbital occupation of the *d*-only model with $U' = 4$ eV, $J = 0.75$ eV ($U = 5.5$ eV), $\beta = 100$ eV$^{-1}$ at quarter-filling ($n_d = 1$) as a function of the initial crystal field splitting $\Delta_{\text{CF}}^d$. The DMFT data (solid symbols) are compared with the corresponding noninteracting results (empty symbols). The arrows indicate the effect of the interaction which is essentially opposite for negative and positive $\Delta_{\text{CF}}^d$. The shaded region on the left indicates the onset of the Mott-Hubbard insulating phase.

asymmetric also in the presence of the interactions, from the data of Fig. 2 we note that, for each orbital, the deviations w.r.t. to the noninteracting values are strongly dependent on $\Delta_{\text{CF}}^d$: The sign of the change in the orbital occupations appears closely connected with the sign of $\Delta_{\text{CF}}^d$. Specifically, for $\Delta_{\text{CF}}^d > 0$ we observe generally an enhancement (reduction) of the occupation of the first (second) $x^2 - y^2$ ($3z^2 - r^2$) orbital, while for $\Delta_{\text{CF}}^d < 0$ the trend is the opposite.

This is reflected in an analogous trend of the change to the orbital polarization $P$, formally defined as in Refs. 38 and 52:

$$P = \frac{n_{x^2-y^2} - n_{3z^2-r^2}}{n_{x^2-y^2} + n_{3z^2-r^2}} \qquad (7)$$

as well as in the Fermi surfaces, shown in Fig. 6. For the latter ones, which will be discussed more extensively in the next section, our DMFT results show that, depending on the sign of the initial orbital splitting ($\Delta_{\text{CF}}^d$), the character (as well as the typical shape) of the Fermi surface corresponding to the lower-energy orbital gets increased by the electronic interaction.

In fact, such trends explain the qualitatively different LDA + DMFT results previously obtained for the shape of the Fermi surface via specific *d*-only calculations for bulk nickelates[20] and Ni-based heterostructures,[18,19] respectively: The difference in the results essentially reflects the different sign of the initial crystal field splitting ($\Delta_{\text{CF}}^d$), as estimated by the *ab initio* calculations, whose final size ($\Delta_{\text{eff}}^d$) gets significantly magnified by the electronic interaction.

The last statement can be formalized more quantitatively through the analysis of the corresponding self-energies presented in Fig. 3: here, we show the differences between the real parts of the DMFT self-energy of the two orbitals, i.e., $\text{Re}\Sigma_{3z^2-r^2}(i\omega_n) - \text{Re}\Sigma_{x^2-y^2}(i\omega_n)$, evaluated in the limit frequency $\omega_n \rightarrow 0$ and $\omega_n \rightarrow +\infty$, respectively. We recall that in the latter limit only the Hartree contributions to the electronic self-energy remain. Hence, the difference between
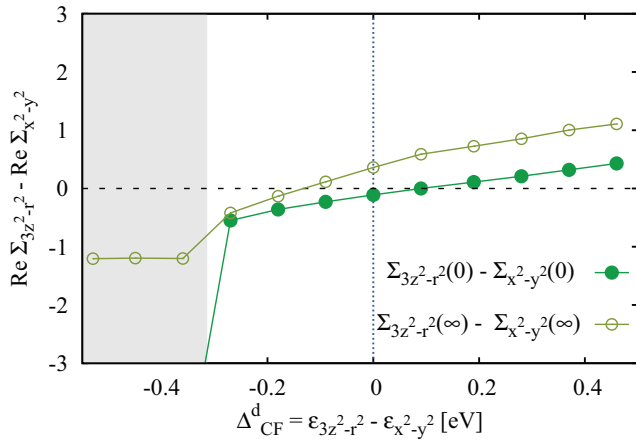
FIG. 3. (Color online) Difference of the real part of the DMFT self-energies for the two orbitals of the $d$-only model with $U' = 4$ eV, $J = 0.75$ eV ($U = 5.5$ eV), $\beta = 100$ eV$^{-1}$ at quarter-filling ($n_d = 1$) extrapolated to $\omega_n \to 0$ (solid symbols) and $\omega_n \to +\infty$ (empty symbol, Hartree contribution to the self-energy) as a function of the initial energy splitting $\Delta^d_{CF}$. The huge enhancement of the difference between the self-energy at $\omega_n \to 0$, and the consequent huge energy shift of the first orbital, marks the onset of the Mott-Hubbard insulating phase (shaded region on the left).

the self-energies can be also explicitly written in terms of the electronic density as

$$\mathrm{Re}\,\Sigma_{3z^2-r^2}(\infty) - \mathrm{Re}\,\Sigma_{x^2-y^2}(\infty)$$
$$= (U - 5J)(n_{x^2-y^2} - n_{3z^2-r^2}) = (U - 5J)\,P. \quad (8)$$

Here, the last equality only holds at quarter-filling where $n_{x^2-y^2} + n_{3z^2-r^2} = 1$. Such a dependence on the (final) electronic density appears evidently in the corresponding data of Fig. 3. The Hartree contribution, evaluated in DMFT, changes sign[53] precisely where the orbital occupations become equal ($P = 0$), i.e., for the negative values of $\Delta_{CF} \sim -0.15$ eV (see Fig. 2). By comparing this to the previous results, it appears that the high-frequency values of the self-energy do not represent the "crucial" parameter. Instead, the trends in the orbital polarization and, therefore, the predicted physics are controlled by the low-frequency behavior of the self-energy: Up to the MIT, the shape of the Fermi surface is determined by the "effective" CF splitting given by

$$\Delta^d_{\mathrm{eff}} = \Delta^d_{CF} + \mathrm{Re}\,\Sigma_{3z^2-r^2}(0) - \mathrm{Re}\,\Sigma_{x^2-y^2}(0), \quad (9)$$

i.e., as the original crystal field corrected by the difference of the real self-energies for $\omega_n \to 0$. This makes the interpretation of the second set of data shown in Fig. 3 very transparent: the sign of $\mathrm{Re}\,\Sigma_{3z^2-r^2}(0) - \mathrm{Re}\,\Sigma_{x^2-y^2}(0)$ follows that of the original crystal field $\Delta^d_{CF}$, and confirms, from the microscopic point of view, the picture of interaction effects *always* magnifying the size of the original crystal field. Of course, such enhancement will depend quantitatively on many factors: For instance, it will be bigger when the system is more correlated. A dramatic enhancement, in particular, is found when the Mott metal-insulator transition is approached, i.e., when $\Delta^d_{CF}$ approaches the shaded area in Fig. 3. Here, the low-energy physics corresponds to an empty (broader) $x^2 - y^2$ orbital and a half-filled (narrower) $3z^2 - r^2$ orbital.
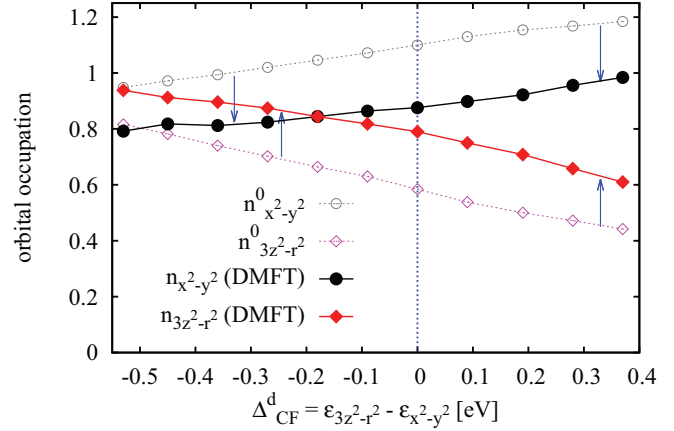


FIG. 4. (Color online) Orbital occupation of the $d$ orbitals as a function of the initial crystal field splitting for the four-band $dp$ model with $U' = 8$ eV, $J = 1.0$ eV ($U = 10$ eV), $\beta = 100$ eV$^{-1}$, and $n_{\mathrm{tot}} = 5$. The DMFT data (solid symbols) are compared with the corresponding noninteracting results (empty symbols).

However, as we will now discuss, these results are contradicted by corresponding calculations performed in larger basis sets, which include also the most relevant $p$ degrees of freedom, as it will be shown explicitly in the next section.

### B. DMFT results for the dp model

For the four-band $dp$ model, the total occupation is $n_{\mathrm{tot}} = n_p + n_d = 5$. Because of the stronger localization of the $d$ orbitals in the $dp$ case, larger values for $U$, $U'$, and $J$ have been considered: We have doubled the value of $U'$ w.r.t. the calculation discussed in the previous section, i.e., $U' = 8$ eV.[54] Because of the smaller screening effects on the Hund's exchange constant, we have considered a reduced enhancement of $J$, which has been fixed to 1 eV. As before, the relation $U = U' - 2J$ holds.

In Fig. 4, we consider first the occupation of the two $d$ orbitals as a function of the initial crystal field splitting, starting from the noninteracting case. Let us recall here that, because of the downfolding procedure, the numerical values of the energy splitting between the $e_g$ orbitals in the one-particle Hamiltonian are evidently different in the $dp$ and in the $d$-only basis sets. They have been labeled, respectively, with $\Delta_{CF}$ [see Eq. (1)] and $\Delta^d_{CF}$. Note that the latter includes, as *ligand* field, the effects of $dp$ hybridization. To allow for a direct comparison to the effective $d$-only results, we have used the relation between $\Delta_{CF}$ and $\Delta^d_{CF}$ and plot the $dp$ results as a function of $\Delta^d_{CF}$.

By analyzing the orbital occupation shown in Fig. 4, the qualitative behavior as a function of $\Delta^d_{CF}$ appears similar as in the $d$-only case. However, an important difference should be noted: In spite of the relatively large separation ($\sim 2$ eV) between $d$ and $p$ bands, the total occupation of the $d$ orbitals is now much larger than before ($n_d \sim 1.7 \div 1.8$) due to the $dp$ hybridization. Quite remarkably, according to our DMFT results of Fig. 4, such an enhanced occupation of the "correlated" $d$ orbitals essentially survives also upon switching on the local interaction. This fact has an obvious impact on the final results for the orbital polarization $P$, as now the
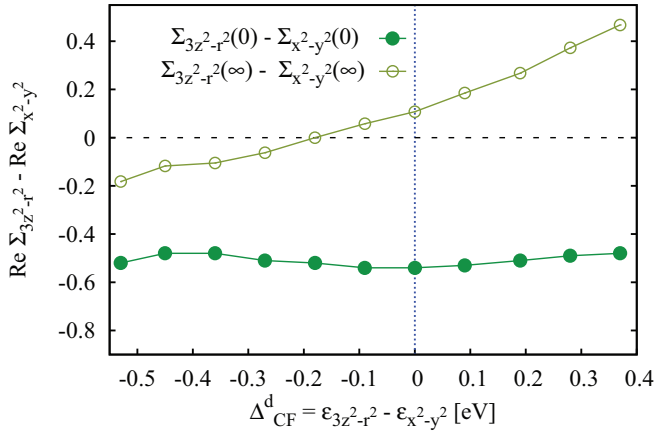
FIG. 5. (Color online) Difference of the real part of the DMFT self-energies for the two $d$ orbitals of the four-band $dp$ model with $U' = 8$ eV, $J = 1$ eV ($U = 10$ eV), $\beta = 100$ eV$^{-1}$, and the filling is $n_{\rm tot} = 5$. Shown are the low- and high-frequency asymptotes, i.e., the extrapolation to $\omega_n \to 0$ (solid symbols) and $\omega_n \to +\infty$ (empty symbol, Hartree contribution to the self-energy).

sign of its change w.r.t. the noninteracting case is no longer related to $\Delta_{\rm CF}^d$: Fig. 4 shows that independently of the sign $\Delta_{\rm CF}^d$, one *always* observes a reduction of the value of $P$, i.e., a net enhancement (reduction) of the occupation of the $3z^2 - r^2$ ($x^2 - y^2$) orbital driven by the electronic interaction.

The analysis of the corresponding self-energies provides a further confirmation: Fig. 5 shows the plot of the zero-frequency extrapolation of the real part of the self-energy (compare to Fig. 3). In contrast to the $d$-only results, now the interaction correction always reduces the initial crystal field, in agreement with the systematic depletion of the $x^2 - y^2$

orbital (reduction of $P$) observed in the whole parameter range considered.

On the basis of these results, it is interesting to examine the consequences for the shape of the Fermi surfaces (FS) in the different cases. In Fig. 6, we show the Fermi surfaces for two different values of $\Delta_{\rm CF}^d$ for both the $d$-only and the $dp$ basis sets. In the upper row, we show the noninteracting result and in the lower row the DMFT one. In particular, the two values of $\Delta_{\rm CF}^d$ have been chosen to present the extreme cases within our data range (provided that the solution is metallic and has a FS). As for the analysis of Fig. 6, we start by considering the noninteracting FS of the upper row for the two different basis sets: as a consequence of the Löwdin downfolding, the shape of noninteracting FS corresponding to the same values of $\Delta_{\rm CF}^d$ coincide, while the orbital character encoded by the colors differs in that the $p$ contribution is explicitly present in the $dp$ case. Additionally, for each case considered, the contribution to the FS of the $3z^2 - r^2$ orbital (encoded by the red color and responsible for the formation of the "cylindric"-shaped FS sheet around the $\Gamma$ point) is stronger for negative values of $\Delta_{\rm CF}^d$ than for positive.

By looking at the DMFT data (lower row) for the $dp$ four-band model, we see that the overall negative correction to $\Delta_{\rm eff}^d$ reported in Fig. 5 gives a definite trend for the Fermi surfaces: In the $dp$ case, the interaction, *independently* of the sign of $\Delta_{\rm CF}^d$, always enhances the $3z^2 - r^2$ contribution. This is reflected both in the orbital composition (the interacting FS contain more red) and in the shape (enlargement of the central FS sheet). At the same time, our DMFT data unveil quite different trends for the interacting FS of the $d$-only model: The $3z^2 - r^2$ contribution is enhanced *only* for $\Delta_{\rm CF}^d < 0$, i.e., only if the $3z^2 - r^2$ was from the beginning the lowest lying of the $e_g$ orbitals. In fact, coherently with the behavior of $\Delta_{\rm eff}^d$
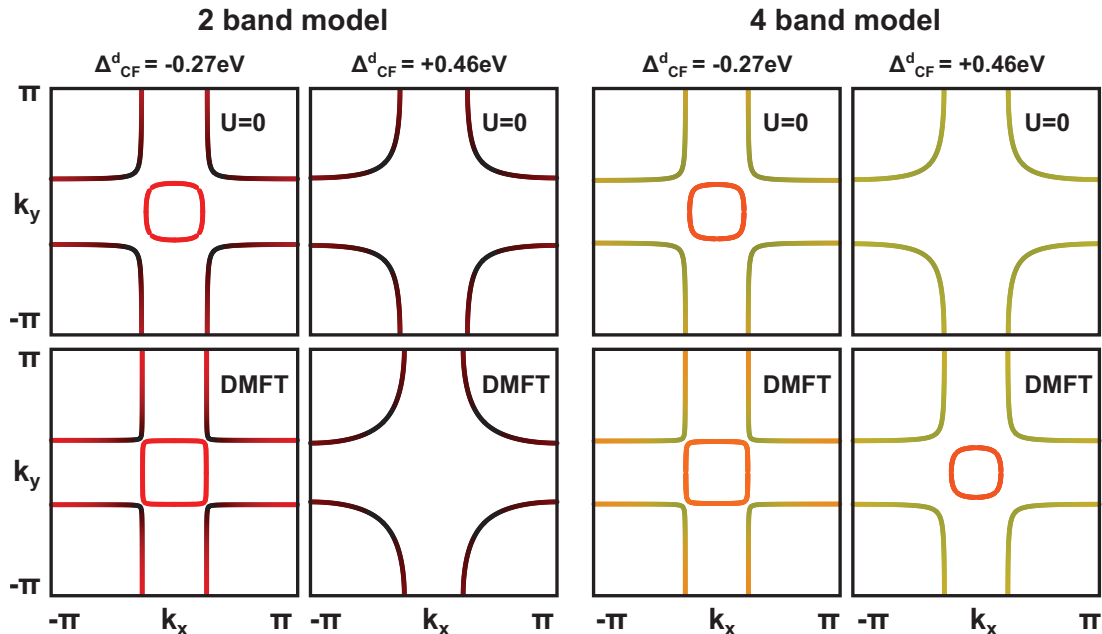


FIG. 6. (Color online) Shape and orbital character of the electronic Fermi surfaces in the two different basis sets (left: $d$-only model; right: $dp$ model). The DMFT results are shown in the upper row and the noninteracting case in the lower row for comparison. The two negative/positive values of $\Delta_{\rm CF}^d$ considered have been chosen as different as possible, with the requirement that a metallic Fermi surface is still found in the interacting case. The color coding of the orbital character [black: $x^2 - y^2$, red: $3z^2 - r^2$, yellow: $p$ orbital(s), is the same as in Fig. 1].
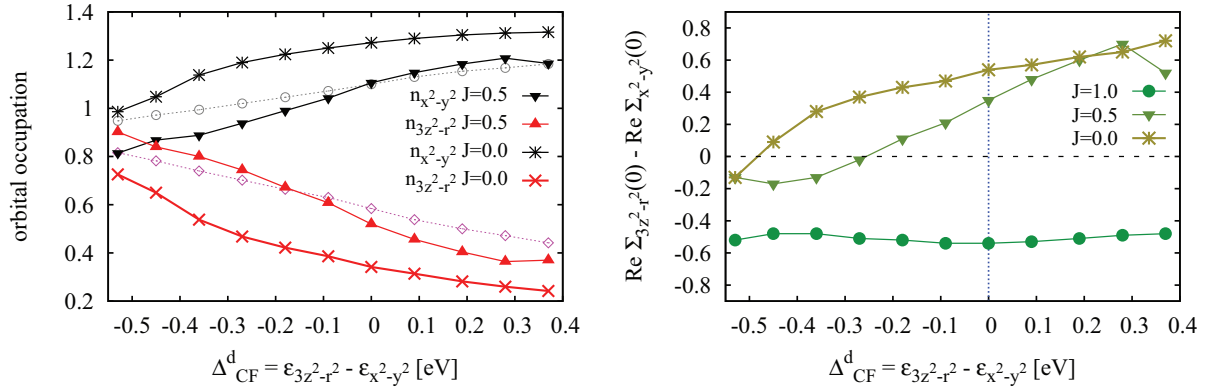
FIG. 7. (Color online) Left panel: Orbital occupation of the $d$ orbitals of the four-band $dp$ model as a function of the initial crystal field splitting $\Delta_{CF}^d$. We used $U' = 8$ eV, $\beta = 100$ eV$^{-1}$, $n_{tot} = 5$, and two different values of the Hund's exchange $J = 0.0, 0.5$ eV. The DMFT data (solid symbols) are compared with the corresponding noninteracting results (empty symbols). Right panel: Corresponding data for the difference of the real part of the DMFT self-energies for the two $d$ orbitals of the four-band $dp$ model extrapolated to $\omega_n \to 0$ as a function of the initial crystal field splitting $\Delta_{CF}^d$. The self-energy data are also compared with the corresponding DMFT data at $J = 1.0$, previously shown in Fig. 5.

(see Fig. 3), for positive values of $\Delta_{CF}^d$, the interaction further reduces the $3z^2 - r^2$ contribution to the FS, which becomes progressively "darker" colored and more "$x^2 - y^2$" shaped. Let us note that, depending on the details of the dispersion of the specific $d$-only problem, there are cases in which for $\Delta_{CF}^d > 0$ the noninteracting FS still presents two sheets, but the reduction of the $3z^2 - r^2$ character predicted by DMFT determines a transition to a single-sheet FS in the interacting case, analogous to the one calculated in Ref. 18.

Summarizing the main outcome of the comparsion of our DMFT calculations in different basis sets for orbital occupations, crystal field corrections, and Fermi surface evolution, an evident *qualitative* disagreement is observed, at least in the region of positive values of the initial crystal field $\Delta_{CF}^d$. It is worth noticing that for positive values of $\Delta_{CF}^d$, the trend we found in the $dp$ basis set is consistent with the results of the $dp$ calculations for the Ni-based heterostructures of Ref. 38: There, it was shown that even when starting from a relatively significant orbital polarization for the $x^2 - y^2$ orbital at the LDA level, the polarization was always strongly reduced by the interaction, which obviously has bad implications on the possibility of actually manipulating the Fermi surfaces of the Ni-based heterostructures in the "desired" cupratelike way.[18,21] As a matter of fact, this discrepancy between $d$-only and $dp$ results has been found here by also including the SU(2) symmetry of the local interaction on the $e_g$ bands in both DMFT calculations. This confirms the hypothesis of Ref. 38 that such a discrepancy in the theoretical predictions does not originate from a different treatment of the interactions between the calculations of Refs. 18,19 and 38, but rather from some more intrinsic difference in the calculations. The most evident systematic difference is the filling $n_d$ of the two $e_g$ orbitals, which, due to the $dp$ hybridization is strongly increased w.r.t. the quarter-filling level of the $d$-only model. While this is rather obvious at the LDA level, we note that the occupation of the $d$ manifold does not change much even in the presence of the interaction, for typical choices of the double-counting term for the DMFT (see Sec. II, for details, and also Ref. 38). Quite interestingly, the possible role of an enhanced $d$-orbital

occupation in $dp$ calculations has been also recently addressed, for the different problem of the occurrence of the MIT.[36]

The point we make here is that the Hund's exchange $J$ has a strikingly different effect in the $d$-only and in the $dp$ models, due to the fact that, close to half-filling, $J$ drives the system very effectively towards the Hund's rule high-spin ground state.[58] For the orbital polarization, this means that $J$ does not play a decisive role for the quarter-filled $d$-only model while it becomes extremely important in the $dp$ model, where $n_d \sim 1.7 \div 1.8$. The $d$ and $dp$ results can indeed be reconciled qualitatively if the Hund's coupling $J$ for the $dp$ model is equal to $\approx 0.5$ eV or smaller. This is shown in Fig. 7, in which the $dp$ calculations have been performed reducing the value of $J$ from 1.0 eV to $J = 0.5$ eV, and $J = 0.0$ eV ($U' = U - 2J = 8$ eV is kept fixed, instead).

The combined analysis of the orbital occupation and of the self-energy (at $\omega_n \to 0$) results shows that the $dp$ results of Figs. 4 and 5 change qualitatively already for the case $J = 0.5$ eV: the overall trend of strong reduction of occupation of the first $x^2 - y^2$ orbital disappears for a large region of values of the initial crystal field $\Delta_{CF}^d$. In fact, the results already at $J = 0.5$ eV would lead to a physical situation which is qualitatively similar to that predicted by the $d$-only model. As one can expect, the change with respect to the previous $dp$ results becomes even larger when setting $J = 0.0$ eV, as both trends of orbital occupation and effective crystal field become exactly opposite, with the $x^2 - y^2$-orbital occupation always increased by the interaction irrespectively of the value of the initial $\Delta_{CF}^d$. The sensitivity of the final $dp$ results on the Hund's coupling is very illustrative and shows the crucial role of the Hund's exchange in this situation.[55]

## IV. RESULTS: THE ROLE OF THE $d$-ORBITAL OCCUPATION

From the marked discrepancy between $dp$ and $d$ results, discussed in the previous section, a general question naturally arises: Under which conditions can one expect to obtain

a qualitatively similar DMFT description of the interaction effects for $d$-only and $dp$ calculations?

Let us assume here that we have a very accurate estimate[59] of the local interactions and especially of the Hund's exchange $J$. One of the most basic differences between the $d$-only and the $dp$ calculations examined is the different value of the occupation of the $d$ orbitals. This difference is observed already at the level of the noninteracting model and is, remarkably, not strongly affected by the inclusion of the interaction: For the $d$-only model, the DMFT calculations have been performed, as usual, at fixed filling, while the value of $d$-orbital occupation for the $dp$ calculations presents moderate oscillations around a much larger value of $n_d \sim 1.75$, quite independently of the parameter set $(U, J, \Delta_{CF}^d)$ considered. Since the filling of the *correlated* orbitals is a crucial factor to drive the system towards a Mott-Hubbard MIT, this will naturally represent one of the key parameters to be considered when comparing LDA + DMFT calculations on different basis sets.

To make our statement more quantitative, we have performed several additional DMFT calculations for the same $d$-only model as in Sec. II, but now varying systematically $n_d$ from the original quarter-filling level up to the much higher $n_d \sim 1.75$ found in the $dp$ calculations. The results for the orbital occupations and the self-energy at the Fermi level are shown in Fig. 8 in the upper and lower row panels, respectively. By gradually increasing the total occupation of the $d$ orbitals, and focusing on the most interesting regime of $\Delta_{CF}^d > 0$, one observes that the parameter region where the crystal field "drives" the final result (i.e., where its magnitude is enhanced

by the interaction), shrinks, being confined to higher and higher values of the initial $\Delta_{CF}^d$.

Looking at the self-energy plot for $n_d = 1.05$, a qualitative change in the trend of the effective crystal field w.r.t. the noninteracting one is found for $\Delta_*^d \sim 0.2$. For $\Delta_{CF}^d < \Delta_*^d$, the trend for the effective crystal field is *opposite* to that observed for quarter-filling, i.e., the original crystal field $\Delta_{CF}^d$ is *reduced* by the interaction. An analogous trend is also observed for the changes in the orbital occupations w.r.t. the noninteracting ones.

By further increasing $n_d$ to 1.25 (second panels of Fig. 8), the threshold $\Delta_*^d$ is already shifted beyond the border of the parameter region considered ($\Delta_*^d > 0.5$). Finally, if one performs the DMFT $d$-only calculations for $n_d = 1.75$, which is roughly similar as in the $dp$ model, one indeed finds a similar behavior as for the $dp$ model: the interaction correction to the crystal field (Fig. 8), overall negative for all positive values of $\Delta_{CF}^d$ considered, resembles that of the $dp$ model in Fig. 5, reflecting the tendency to deplete the $x^2 - y^2$ orbital in the presence of the electronic interaction.

For a more general analyis of our data in the whole range of $\Delta_{CF}^d$, let us first recall that, due to the different bandwidths of the two $e_g$ orbitals, no symmetric behavior between the regions of positive and negative $\Delta_{CF}^d$ can be expected. In particular, in the region $\Delta_{CF}^d < 0$ (i.e., the less relevant one in the perspective of the Ni-based heterostructures), the crystal field "enhancement" at quarter-filling was much larger than the corresponding one for $\Delta_{CF}^d > 0$ (see Fig. 3), also as an effect of the closer proximity of the MIT in this parameter
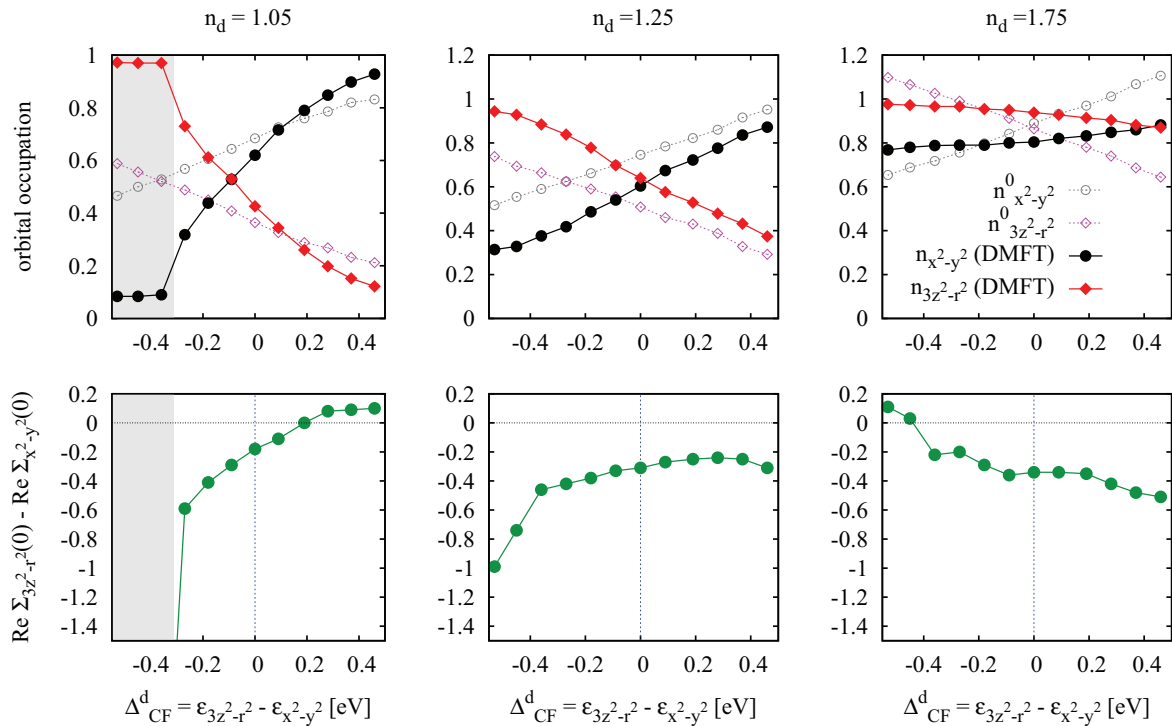


FIG. 8. (Color online) Upper row: Orbital occupations of the two orbitals of the $d$-only model with $U' = 4$ eV, $J = 0.75$ eV ($U = 5.5$ eV), $\beta = 100$ eV$^{-1}$ for different filling $n_d = 1.05, 1.25, 1.75$ as a function of the initial crystal field splitting $\Delta_{CF}^d$. The DMFT data (solid symbols) are compared with the corresponding noninteracting results (empty symbols). Note that a filling of $n_d = 1.75$ roughly corresponds to the filling of the two $d$ orbitals in the $dp$ models considered in the previous sections. Lower row: Difference of the real part of the DMFT self-energies for the two orbitals extrapolated at $\omega_n \to 0$ (solid symbols) as a function of the initial crystal field splitting $\Delta_{CF}^d$ for the corresponding set of data.

region. Hence, while the effects of an increased $n_d$ are always at work, here they become first visible as a gradual weakening of the quarter-filling trends (e.g., as a mitigation of the strongly negative correction to the effective crystal field for $\Delta_{\text{CF}}^d < 0$), before getting to an inversion of them: The gray shadow area, marking the onset of the MIT for one of the two orbitals i.e., the (almost) half-filled one, is shrinking in the $n_d = 1.05$ plot, and essentially disappears at $n_d = 1.25$. Only at higher densities one eventually observes a (weak) sign change of the effective crystal field correction at the lowest border of the parameter region considered ($\Delta_{\text{CF}}^d \sim -0.5$).

These results demonstrate the essential role played by the density of the $d$ manifold for determining the final DMFT results on different basis sets, at least for the important aspect of the Fermi level properties. The starting value of $n_d$ will decide if, *given a correct ab initio estimate* of the interaction parameters of the multiorbital Hubbard Hamiltonian, the physics of the interacting system will be *driven* by the (original) crystal field, or rather by the Hund's rule tendency for equally occupied orbitals. Therefore, it will be *a priori* quite hard to reconcile DMFT calculations performed on different basis sets, without considering the corresponding occupation of the *correlated* manifolds.

From the perspective of actual material calculations, the strong dependence of the final LDA + DMFT results for the Ni-based heterostructures can be put in a rather general framework. In fact, the quarter-filling physics particularly favors the crystal field dominated physics since the Hund's exchange is weaker in a system with one electron (on average). Hence, if the $dp$ hybridization can drive the system away from this regime (as is the $dp$ model considered here with an average filling of $n_d \sim 1.75$), the Hund's exchange will easily prevail over the crystal field effects. The same interpretation can likely explain why the results of LDA + DMFT calculations for the Fe-based superconductors do not display, in most cases, such crucial dependence on the basis set considered. There, the five orbitals of the Fe $3d$ manifold are characterized by a small value of the *overall* orbital energy splitting $\sim 0.2$ eV (in comparison to the typical values of the order of 1 eV observed in many transition-metal oxides). This corresponds to a situation of *five* partially filled [$n_d \sim 6$ (Ref. 61)] correlated orbitals all very close energetically to the Fermi level, i.e., one of the most favorable playgrounds for strong Hund's exchange processes. Hence, this case is well inside one of the two regimes, and moderate differences in the orbital occupation of the $d$ manifold in different basis sets will *not* result in a qualitative discrepancy between different LDA + DMFT calculations, with the possible exception of the regimes closest to the Mott transitions.[62,64,65]

## V. CONCLUSIONS

We have thoroughly compared two models for transition-metal oxides: a $d$-only model containing two effective $d$ orbitals and a $dp$ model made of two $d$ and two $p$ orbitals. On the single-particle level without Coulomb interaction, the two models show the same low-energy physics and band structure. However, if the Coulomb interaction is taken into account by means of DMFT, this is not the case any more.

The main reason for this discrepancy is the number of $d$ electrons. In the $d$-only model, there is on average one $d$ electron per site. For the $dp$ model, on the other hand, the bands are filled with altogether five electrons per site: Without hybridization, the two $p$ orbitals at lower energy would be completely filled, and the $d$ orbitals in the vicinity of the Fermi level would have the same filling (one electron per site) as for the $d$-only model. The $d$ orbitals hybridize, however, with the $p$ orbitals, and, hence, there is some admixture between the orbitals leading to a larger filling ($\sim 1.7$) of the $d$ orbitals for the $dp$ model.

This different filling has dramatic consequences for the correlated solution of the two models. For the $d$-only model, the Coulomb interaction enhances the initial crystal field splitting, leading to a situation with one $d$ electron in the lowest-lying $d$ orbital. Depending on the original crystal field (e.g., if $\Delta_{\text{CF}}^d > 0$), this can be the $x^2 - y^2$ orbital, which hence dominates the low-energy physics and Fermi surface topology. This kind of physics can result in a very similar $x^2 - y^2$-shaped Fermi surface in Ni-based heterostructures as in cuprates.

In contrast, in the $dp$ model the Hund's exchange favors a more even occupation of the two orbitals because the $d$ manifold is much closer to half-filling ($n_d = 2$). The initial crystal field splitting is therefore reduced and the local moment enhanced.[58,66,67] However, if $J$ is low enough, this tendency can be weakened recovering qualitatively the results of the $d$-only model (see Fig. 7).

Vice versa, we have also verified that the $d$-only model displays a similar Hunds physics as that of the $dp$ model, if we enhance the $d$-electron occupation towards the one of the $dp$ model. Let us stress that, while an influence of the filling of the correlated manifold on the DMFT results is not surprising in itself, our study identifies its crucial importance for the description of the low-energy physics. In particular, two important aspects have been determined: (i) the rapidity with which qualitative robust trends found in the $d$-only basis sets can be reversed by slightly varying the density from the "nominal" one (e.g, from $n_d = 1$ in our case), and (ii) the similarity of the interaction effects in different basis sets observed in the presence of a correspondingly similar occupation of the correlated orbitals.

The findings of our model study have important consequences for the analysis and the interpretation of realistic LDA + DMFT calculations for several transition-metal oxides and related correlated materials: The physical results for $d$-only LDA + DMFT calculations can indeed dramatically differ from calculations which also include the oxygen $p$ orbitals. In fact, since the additional $p$ orbitals lead to a different $d$ filling, this can determine the aforementioned dramatically different low-energy DMFT physics. Eventually, in the case of contradicting DMFT prediction, experiments (such as, e.g., ARPES or x-ray absorption spectroscopy or orbital reflectometry) will show which of the two theoretical setups describes the physical reality better.

Furthermore, we should note that, as the $dp$ calculation is generally far away from an integer filling of the interacting $d$ orbitals, the occurrence of Mott-Hubbard metal-insulator transitions becomes more difficult.[35,36] Certainly, one can expect nonlocal correlations beyond DMFT (Ref. 37) to be of importance for (quasi-) two-dimensional Mott insulators.

However, not showing a Mott insulating phase in other specific cases might well be a deficit of the $dp$ calculations or, at least, of the way such $dp$ calculations are performed nowadays, e.g., via the complete neglect of the $dp$ interaction.

Let us emphasize, finally, that in other situations the physics of the $d$-only and $dp$ calculations can be much more similar. This was, e.g., observed in most of the DMFT studies on iron pnictides. In these materials, the presence of a large manifold of partially filled correlated $3d$ orbitals all close to the Fermi level is a common aspect for both $dp$ and $d$-only calculations. Hence, in both cases, the physics is mostly dominated[14,62] by Hund's rule forming a large local magnetic moment in a correlated metallic environment.

[1] J. Hubbard, Proc. R. Soc. London, Ser. A **276**, 238 (1963); M. C. Gutzwiller, Phys. Rev. Lett. **10**, 159 (1963); J. Kanamori, Prog. Theor. Phys. **30**, 275 (1963).

[2] W. Metzner and D. Vollhardt, Phys. Rev. Lett. **62**, 324 (1989).

[3] A. Georges, G. Kotliar, W. Krauth, and M. Rozenberg, Rev. Mod. Phys. **68**, 13 (1996).

[4] V. I. Anisimov, A. I. Poteryaev, M. A. Korotin, A. O. Anokhin, and G. Kotliar, J. Phys.: Condens. Matter **9**, 7359 (1997); A. I. Lichtenstein and M. I. Katsnelson, Phys. Rev. B **57**, 6884 (1998); G. Kotliar, S. Y. Savrasov, K. Haule, V. S. Oudovenko, O. Parcollet, and C. A. Marianetti, Rev. Mod. Phys. **78**, 865 (2006); K. Held, Adv. Phys. **56**, 829 (2007).

[5] N. F. Mott, Rev. Mod. Phys. **40**, 677 (1968); *Metal-Insulator Transitions* (Taylor & Francis, London, 1990); F. Gebhard, *The Mott Metal-Insulator Transition* (Springer, Berlin, 1997).

[6] K. Held, G. Keller, V. Eyert, D. Vollhardt, and V. I. Anisimov, Phys. Rev. Lett. **86**, 5345 (2001).

[7] S. Y. Savrasov, G. Kotliar, and E. Abrahams, Nature (London) **410**, 793 (2001).

[8] A. I. Lichtenstein, M. I. Katsnelson, and G. Kotliar, Phys. Rev. Lett. **87**, 067205 (2001).

[9] K. Held, A. K. McMahan, and R. T. Scalettar, Phys. Rev. Lett. **87**, 276404 (2001).

[10] M. Capone, M. Fabrizio, C. Castellani, and E. Tosatti, Science **296**, 2364 (2002).

[11] K. Byczuk, M. Kollar, K. Held, Y.-F. Yang, I. A. Nekrasov, T. Pruschke, and D. Vollhardt, Nat. Phys. **3**, 168 (2007).

[12] A. Toschi, M. Capone, C. Castellani, and K. Held, Phys. Rev. Lett. **102**, 076402 (2009).

[13] K. Haule, J. H. Shim, and G. Kotliar, Phys. Rev. Lett. **100**, 226402 (2008); L. Craco, M. S. Laad, S. Leoni, and H. Rosner, Phys. Rev. B **78**, 134511 (2008).

[14] K. Haule and G. Kotliar, New J. Phys. **11**, 025021 (2009); P. Hansmann, R. Arita, A. Toschi, S. Sakai, G. Sangiovanni, and K. Held, Phys. Rev. Lett. **104**, 197002 (2010); A. Toschi, R. Arita, P. Hansmann, G. Sangiovanni, and K. Held, Phys. Rev. B **86**, 064411 (2012); N. Lanatá, H. U. R. Strand, G. Giovannetti, B. Hellsing, L. de' Medici, and M. Capone, *ibid.* **87**, 045122 (2013).

[15] A. Valli, G. Sangiovanni, O. Gunnarsson, A. Toschi, and K. Held, Phys. Rev. Lett. **104**, 246402 (2010).

[16] M. Potthoff and W. Nolting, Phys. Rev. B **60**, 7834 (1999).

[17] S. Okamoto, Phys. Rev. Lett. **101**, 116807 (2008).

[18] P. Hansmann, Xiaoping Yang, A. Toschi, G. Khaliullin, O. K. Andersen, and K. Held, Phys. Rev. Lett. **103**, 016401 (2009).

[19] P. Hansmann, A. Toschi, Xiaoping Yang, O. K. Andersen, and K. Held, Phys. Rev. B **82**, 235123 (2010).

[20] M. Uchida, K. Ishizaka, P. Hansmann, Y. Kaneko, Y. Ishida, X. Yang, R. Kumai, A. Toschi, Y. Onose, R. Arita, K. Held, O. K. Andersen, S. Shin, and Y. Tokura, Phys. Rev. Lett. **106**, 027001 (2011); M. Uchida, K. Ishizaka, P. Hansmann, X. Yang, M. Sakano, J. Miyawaki, R. Arita, Y. Kaneko, Y. Takata, M. Oura, A. Toschi, K. Held, A. Chainani, O. K. Andersen, S. Shin, and Y. Tokura, Phys. Rev. B **84**, 241109 (2011).

[21] J. Chaloupka and G. Khaliullin, Phys. Rev. Lett. **100**, 016404 (2008).

[22] We note that such an enhanced crystal field splitting in DMFT has been first observed in realistic calculations for $V_2O_3$ (Ref. 23) as well as in model multiorbital studies (Ref. 24).

[23] G. Keller, K. Held, V. Eyert, D. Vollhardt, and V. I. Anisimov, Phys. Rev. B **70**, 205116 (2004); A. I. Poteryaev, J. M. Tomczak, S. Biermann, A. Georges, A. I. Lichtenstein, A. N. Rubtsov, T. Saha-Dasgupta, and Ole K. Andersen, *ibid.* **76**, 085127 (2007).

[24] A. I. Poteryaev, M. Ferrero, A. Georges, and O. Parcollet, Phys. Rev. B **78**, 045115 (2008).

[25] P. Hansmann, Ph.D. thesis, Vienna University of Technology, Austria, 2010.

[26] G. H. Wannier, Rev. Mod. Phys. **34**, 645 (1962); N. Marzari and D. Vanderbilt, Phys. Rev. B **56**, 12847 (1997).

[27] O. K. Andersen, *Electronic Structure and Physical Properties of Solids: The Uses of the LMTO Method*, Lecture Notes in Physics (Springer, New York, 2000).

[28] For examples of typical Wannier functions in different basis sets, see M. W. Haverkort, M. Zwierzycki, and O. K. Andersen, Phys. Rev. B **85**, 165113 (2012).

[29] J. Kuneš, V. I. Anisimov, S. L. Skornyakov, A. V. Lukoyanov, and D. Vollhardt, Phys. Rev. Lett. **99**, 156404 (2007).

[30] J. Kuneš, L. Baldassarre, B. Schächner, K. Rabia, C. A. Kuntscher, Dm. M. Korotin, V. I. Anisimov, J. A. McLeod, E. Z. Kurmaev, and A. Moewes, Phys. Rev. B **81**, 035122 (2010).

[31] A. Perucchi, C. Marini, M. Valentini, P. Postorino, R. Sopracase, P. Dore, P. Hansmann, O. Jepsen, G. Sangiovanni, A. Toschi, K. Held, D. Topwal, D. D. Sarma, and S. Lupi, Phys. Rev. B **80**, 073101 (2009).

[32] J. Kuneš, V. Křápek, N. Parragh, G. Sangiovanni, A. Toschi, and A. V. Kozhevnikov, Phys. Rev. Lett. **109**, 117206 (2012).

[33] V. Křápek, P. Novák, J. Kuneš, D. Novoselov, Dm. M. Korotin, and V. I. Anisimov, Phys. Rev. B **86**, 195104 (2012).

[34]M. Aichhorn, L. Pourovskii, V. Vildosola, M. Ferrero, O. Parcollet, T. Miyake, A. Georges, and S. Biermann, Phys. Rev. B **80**, 085101 (2009); S. L. Skornyakov, A. V. Efremov, N. A. Skorikov, M. A. Korotin, Yu. A. Izyumov, V. I. Anisimov, A. V. Kozhevnikov, and D. Vollhardt, *ibid.* **80**, 092501 (2009); S. L. Skornyakov, A. A. Katanin, and V. I. Anisimov, Phys. Rev. Lett. **106**, 047007 (2011); M. Aichhorn, L. Pourovskii, and A. Georges, Phys. Rev. B **84**, 054529 (2011).

[35]K. Held, http://online.kitp.ucsb.edu/online/cem02/held.

[36]X. Wang, M. J. Han, L. de' Medici, H. Park, C. A. Marianetti, and A. J. Millis, Phys. Rev. B **86**, 195136 (2012).

[37]T. Maier *et al.*, Rev. Mod. Phys. **77**, 1027 (2005); G. Kotliar, S. Y. Savrosov, G. Palsson, and G. Biroli, Phys. Rev. Lett. **87**, 186401 (2001); A. I. Lichtenstein and M. I. Katsnelson, Phys. Rev. B **62**, R9283 (2000); A. Toschi, A. A. Katanin, and K. Held, *ibid.* **75**, 045118 (2007); A. N. Rubtsov, M. I. Katsnelson, and A. I. Lichtenstein, *ibid.* **77**, 033101 (2008); G. Rohringer, A. Toschi, H. Hafermann, K. Held, V. I. Anisimov, and A. A. Katanin, *ibid.* **88**, 115112 (2013).

[38]M. J. Han, Xin Wang, C. A. Marianetti, and A. J. Millis, Phys. Rev. Lett. **107**, 206804 (2011); **110**, 179904(E) (2013).

[39]F. Lechermann, S. Biermann, and A. Georges, Prog. Theor. Phys. Suppl. **160**, 233 (2005).

[40]Note: The completely filled $t_{2g}$ orbitals can affect the broadening of the corresponding high-frequency part of the photoemission spectra, but *not* the low-energy electronic structures close to the Fermi level (Ref. 44).

[41]P. Löwdin, J. Chem. Phys. **19**, 1396 (1951).

[42]See, also, O. K. Andersen, in *Correlated Electrons: From Model to Metals*, Lecture Notes of the Autumn School Correlated Electrons 2012, edited by E. Pavarini, E. Koch, F. Anders, and M. Jarrell (Forschungszentrum Jülich GmbH, Zentralbibliothek, Verlag, 2012), Chap. 3, pp. 26–27.

[43]O. K. Andersen, A. I. Lichtenstein, O. Jepsen, and F. Paulsen, J. Phys. Chem. Solids **56**, 1573 (1995).

[44]X. Deng, M. Ferrero, J. Mravlje, M. Aichhorn, and A. Georges, Phys. Rev. B **85**, 125137 (2012).

[45]Geometrically, it corresponds to a tetragonal distortion, a compression or elongation along one of the cubic $C^4$ axes, of the ligand octahedron.

[46]V. I. Anisimov, J. Zaanen, and O. K. Andersen, Phys. Rev. B **44**, 943 (1991).

[47]M. Karolak, G. Ulm, T. O. Wehling, V. Mazurenko, A. Poteryaev, and A. I. Lichtenstein, J. Electron Spectrosc. Relat. Phenom. **181**, 11 (2010).

[48]P. Werner and A. J. Millis, Phys. Rev. B **74**, 155107 (2006).

[49]E. Gull, A. J. Millis, A. I. Lichtenstein, A. N. Rubtsov, M. Troyer, and P. Werner, Rev. Mod. Phys. **83**, 349 (2011).

[50]K. Haule, Phys. Rev. B **75**, 155113 (2007).

[51]N. Parragh, A. Toschi, K. Held, and G. Sangiovanni, Phys. Rev. B **86**, 155158 (2012).

[52]E. Benckiser and M. Haverkort *et al.*, Nat. Mater. **10**, 189 (2011).

[53]Note that the sign of the Hartree difference depends also on the value of the Hund's exchange $J$ (see also Ref. 39). However, for plausible values of $J$, the condition $U > 5J$ is typically fulfilled, and, hence, the sign prefactor in Eq. (8) can be usually assumed as positive.

[54]Note that the trends emerging from our analysis have been tested to be quite stable against the changes of $U$, in a relatively broad range, while they are more sensible to changes of the Hund's exchange $J$, as discussed in the text.

[55]We note that the important physics driven by the Hund's exchange processes has attracted a considerable interest in the most recent literature (Refs. 56–58).

[56]P. Werner, E. Gull, M. Troyer, and A. J. Millis, Phys. Rev. Lett. **101**, 166405 (2008).

[57]A. Georges, L. de' Medici, and J. Mravlje, Annu. Rev. Condens. Matter Phys. **4**, 137 (2013).

[58]L. de' Medici, Phys. Rev. B **83**, 205112 (2011); L. de' Medici, J. Mravlje, and A. Georges, Phys. Rev. Lett. **107**, 256401 (2011).

[59]For example, from constrained cRPA or even for cRPA locally unscreened calculations (Ref. 60).

[60]Y. Nomura, M. Kaltak, K. Nakamura, C. Taranto, S. Sakai, A. Toschi, R. Arita, K. Held, G. Kresse, and M. Imada, Phys. Rev. B **86**, 085117 (2012).

[61]See, e.g., the LDA + DMFT systematic study of Fe 3$d$ occupation in Ref. 62. We note, though, that higher occupation values have been recently reported in Ref. 63.

[62]Z. P. Yin, K. Haule, and G. Kotliar, Nat. Mater. **10**, 932 (2011).

[63]T. Schickling, F. Gebhard, J. Bünemann, L. Boeri, O. K. Andersen, and W. Weber, Phys. Rev. Lett. **108**, 036406 (2012).

[64]L. de' Medici, G. Giovannetti, and M. Capone, arXiv:1212.3966.

[65]F. Hardy, A. E. Böhmer, D. Aoki, P. Burger, T. Wolf, P. Schweiss, R. Heid, P. Adelman, Y. X. Yao, G. Kotliar, J. Schmalian, and C. Meingast, Phys. Rev. Lett. **111**, 027002 (2013).

[66]P. Werner and A. J. Millis, Phys. Rev. Lett. **99**, 126405 (2007); M. Sentef, J. Kuneš, P. Werner, and A. P. Kampf, Phys. Rev. B **80**, 155116 (2009).

[67]J. C. Budich, B. Trauzettel, and G. Sangiovanni, Phys. Rev. B **87**, 235104 (2013).